^{23}Na Relaxation in Isotropic and Anisotropic Liquid-Crystalline DNA Solutions

Leonore C. A. Groot, Johan R. C. van der Maarel, and Jaap C. Leyte*

Gorlaeus Laboratories, Department of Physical and Macromolecular Chemistry, University of Leiden, P.O. Box 9502, 2300 RA Leiden, The Netherlands

*Received: July 27, 1993; In Final Form: December 21, 1993**

The ^{23}Na relaxation in isotropic and anisotropic aqueous, salt-free DNA fragment (500 Å) solutions is investigated. The temperature dependence of the coupling constants and correlation times are reported. Premelting effects occur in the isotropic phase, whereas this is not observed in the anisotropic solution. Slow dynamic processes in the frequency range 200–9000 Hz are absent in both phases.

Introduction

Persistence length (500 Å) DNA fragment solutions undergo a series of phase transitions as the concentration is raised. Several studies regarding the influence of temperature and added low molecular weight salt on the phase behavior have been performed.[1-4] Polarized light microscopy as well as ^{31}P and ^{23}Na NMR relaxation experiments are the most commonly used techniques to study this behavior. ^{23}Na NMR relaxation experiments are also very useful to study the dynamical processes in these solutions. For the isotropic phase, this has been reported a few years ago.[5] Premelting effects were observed and local concentrical diffusion of the counterions around the DNA molecules as well as the internal motions of the DNA helices were concluded to be the most likely causes of relaxation.

Above a certain concentration, persistence length DNA fragment solutions become cholesteric. In a cholesteric liquid crystal the DNA molecules arrange parallel to each other in a plane. The average direction of the ordered molecules is indicated by the direction. In each consecutive plane, the director is tilted over a certain angle, so macroscopically a cholesteric structure appears. The pitch of this helix is of the order the wavelength of visible light. To see if this tremendous change in solution structure is of any influence on the dynamical processes that drive nuclear relaxation, the dynamic behavior of both the isotropic and the anisotropic phase has presently been investigated in the temperature range from 278 to 303 K.

Coupling constants and correlation times of both solutions are presented and several dynamical processes that occur in the isotropic and the anisotropic phase are discussed. The premelting behavior in both phases is compared.

Theory

The spin dynamics of a spin $^3/_2$ nucleus (e.g., ^{23}Na) is sensitive to the interaction of the electric quadrupole moment with electric field gradients generated by the surrounding medium. The average value of the electric field gradient causes a quadrupole splitting of the magnetic resonance, whereas the fluctuations induce relaxation.

In an isotropic solution, the average value of the electric field gradient equals zero. In an anisotropically ordered medium, e.g., a liquid crystal, a static electric field gradient may cause a splitting of the NMR frequency spectrum. Apart from this splitting, the presence of a nonzero electric field gradient has a profound influence on the spin $^3/_2$ relaxation behavior. Therefore, both cases will be described separately.

Under motional averaging conditions and zero average electric field gradient, the spin $^3/_2$ relaxation behavior has been detailed many years ago by Hubbard.[6] In this isotropic case the relation between the measured longitudinal relaxation rate and the spectral densities is given by

$$M_z(t) - M_0 = M_0[0.2\exp(-R_{1f}\cdot t) + 0.8\exp(-R_{1s}\cdot t)] \quad (1)$$

with

$$R_{1f} = 2\left[\frac{eQ}{\hbar}\right]^2 J_1(\omega_0), \quad R_{1s} = 2\left[\frac{eQ}{\hbar}\right]^2 J_2(2\omega_0) \quad (2)$$

For the transverse relaxation, this relation reads

$$M_{xy}(t) = M_0[0.6\exp(-R_{2f}\cdot t) + 0.4\exp(-R_{2s}\cdot t)] \quad (3)$$

with

$$R_{2f} = \left[\frac{eQ}{\hbar}\right]^2 [J_0(0) + J_1(\omega_0)],$$

$$R_{2s} = \left[\frac{eQ}{\hbar}\right]^2 [J_1(\omega_0) + J_2(2\omega_0)] \quad (4)$$

Outside the extreme narrowing limit, both the longitudinal and the transverse relaxation rates are biexponential and characterized by a fast (R_{1f}, R_{2f}) and a slow (R_{1s}, R_{2s}) relaxation rate. In these equations M_z is the magnetization along the external magnetic field axis, M_{xy} is the magnetization perpendicular to this axis, and M_0 is the equilibrium magnetization. The spectral density at m times the Larmor frequency ω_0 is denoted by $J_m(m\omega_0)$ and will be detailed below. The other symbols have their usual meanings.

In the absence of a static quadrupole splitting, the low-frequency behavior of the spectral density can be investigated using the multiple-pulse $(\pi/2)_\varphi - [T/2 - (\pi/2)_{\varphi-\pi/2} - T/2]_n$ quadrupole echo experiment.[7] If the signal is sampled between the $(\pi/2)$ pulses, the relaxation is given by

$$M_q(t) = 0.8\exp(-R_{qf}\cdot t) + 0.2\exp(-R_{qs}\cdot t) \quad (5)$$

with

$$R_{qf} = \left[\frac{eQ}{\hbar}\right]^2 [0.75J_{20}(T) + J_1(\omega_0) + 0.25J_2(2\omega_0)] \quad (6)$$

$$R_{qs} = \left[\frac{eQ}{\hbar}\right]^2 [J_1(\omega_0) + J_2(2\omega_0)] \quad (7)$$

in which R_{qf} contains the spectral density $J_{20}(T)$. This spectral density depends on the cycle time T, provided the time scale of the fluctuating interaction is of the same order of magnitude. If the spectral density does not show a dispersion in the corresponding frequency range, $J_{20}(T)$ equals the spectral density at zero frequency $J_0(0)$. For a full description of $J_{20}(T)$, the reader is referred to ref 7.

* Abstract published in *Advance ACS Abstracts*, February 1, 1994.

0022-3654/94/2098-2699$04.50/0

In an anisotropic liquid-crystalline sample, the ^{23}Na resonance shows a quadrupole splitting due to the static quadrupole Hamiltonian:

$$H_Q = {}^1/_6\omega_Q(3I_z^2 - I\cdot I) \tag{8}$$

Here, ω_Q is the static quadrupole interaction parameter and the other symbols have their usual meanings. The conventional sodium spectrum consists of a central peak at the resonance frequency ω_0, flanked by two satellites at frequencies $\omega_0 \pm \omega_Q$. As a result of this splitting, one can determine the relaxation rates of both the central peak and the satellites.[8] Provided ω_Q is much larger than the line widths, for the longitudinal relaxation of the central peak (superscript c), one has

$$M_z^c(t) - M_0^c = M_0^c[0.5\exp(-R_{1f}^c t) + 0.5\exp(-R_{1s}^c\cdot t)] \tag{9}$$

with

$$R_{1f}^c = 2\left[\frac{eQ}{\hbar}\right]^2 J_1(\omega_0),\quad R_{1s}^c = 2\left[\frac{eQ}{\hbar}\right]^2 J_2(2\omega_0) \tag{10}$$

The corresponding transverse magnetization relaxes according to

$$M_{xy}^c(t) = M_0^c\exp(-R_2^c\cdot t) \tag{11}$$

with

$$R_2^c = \left[\frac{eQ}{\hbar}\right]^2[J_1(\omega_0) + J_2(2\omega_0)] \tag{12}$$

The longitudinal relaxation rate of the satellite peaks (superscript s) is given by

$$M_z^s(t) - M_0^s = M_0^s\exp(-R_1^s\cdot t) \tag{13}$$

with

$$R_1^s = 2\left[\frac{eQ}{\hbar}\right]^2 J_2(2\omega_0) \tag{14}$$

and for the corresponding transverse relaxation, one has

$$M_{xy}^s(t) = M_0^s\exp(-R_2^s\cdot t) \tag{15}$$

with

$$R_2^s = \left[\frac{eQ}{\hbar}\right]^2[J_0(0) + J_1(\omega_0) + J_2(2\omega_0)] \tag{16}$$

The latter rate contains the spectral density at zero frequency and, hence, is sensitive to slow motion.

The spectral density at m times the Larmor frequency reads

$$J_m(m\omega_0) = {}^1/_2\int[\langle F_{2m}^*(t)F_{2m}(t-\tau)\rangle - \langle F_{2m}^*\rangle^2]\exp(im\omega_0\tau)\,d\tau \tag{17}$$

The spectral density is the Fourier transform of the time correlation function of the electric field gradient (efg) tensor F_{2m} in the laboratory frame minus the square of its mean value. This tensor is defined according to $F_{20} = {}^1/_2V_{zz}$, $F_{2\pm1} = \mp(V_{xz} \pm iV_{yz})/\sqrt{6}$ and $F_{2\pm2} = (V_{xx} - V_{yy} \pm 2iV_{xy})/2\sqrt{6}$.

In the isotropic case the average value of the efg is zero, so the second term of the integral vanishes. Moreover, in this situation the efg correlation function is isotropic with respect to the laboratory frame, and, hence, independent of the index m. In an anisotropic medium, the second term in eq 17 is nonzero. This resulting static electric field gradient is the cause of the quadrupole splitting of the ^{23}Na signal. Now, in a macroscopically oriented sample, the correlation function may depend on the spatial orientation of the efg tensor with respect to the magnetic field. However, in the present work, there is no indication of this effect and, thus, it will be neglected.

In the case of a single-exponential decay of the correlation function, the reduced spectral density will be of Lorentzian form

$$\tilde{J}(\omega) = \frac{2\tau}{1 + \omega^2\tau^2} \tag{18}$$

This reduced spectral density is related to the aforementioned spectral density by

$$\left[\frac{eQ}{\hbar}\right]^2 J(\omega) = \frac{\pi^2}{10}\left\langle\left[\frac{e^2qQ}{\hbar}\right]^2\right\rangle\tilde{J}(\omega) = \frac{\pi^2}{10}\langle\chi^2\rangle\tilde{J}(\omega) \tag{19}$$

where $\langle\chi^2\rangle$ is the mean-square quadrupole coupling constant.

If several independent processes i contribute to the loss of correlation, the spectral density can be written as a sum of Lorentzians:

$$\left[\frac{eQ}{\hbar}\right]^2 J(\omega) = \frac{\pi^2}{10}\sum_i\langle\chi_i^2\rangle\tilde{J}_i(\omega) \tag{20}$$

A possible distribution of the static quadrupolar coupling constant can be investigated using the quadrupolar echo pulse sequence.[9] The main feature of this experiment is the delayed acquisition of the fid after the $(\pi/2)$ pulse pair. Due to this delayed acquisition, satellite signals appear at $\omega_1 = 0$ in the $F(\omega_1)$-dimension (i.e., the Fourier transform with respect to the evolution time).[10] As detailed in ref 9, these signals are essentially free of line broadening due to an inhomogeneous ω_Q and their widths are given by R_2^s/π, with R_2^s given by eq 16.

Experimental Section

DNA fragments were obtained by a micrococcal nuclease digestion of chicken erythrocyte nucleosome core DNA, following the procedure described by Shindo et al.[11] After precipitation in ethanol the material was dried in a vacuum oven (293 K, p = 150 Pa). The DNA was brought to the salt free sodium form by dissolving it in a NaCl solution (0.1 M NaCl, 0.015 M nucleotides/L) and extensive dialysis against pure water. Care was taken that the DNA concentration did not reach values below 0.003 M nucleotides/L. Water was deionized and filtered by a Millipore water purification system (Millipore Co.) and its conductivity did not exceed $1 \times 10^{-6}\ \Omega^{-1}\ cm^{-1}$. The final product was freeze-dried and stored at 255 K.

To determine the DNA fragment molecular weight distribution, gel permeation chromatography has been performed.[12] Some low molecular weight material was present, but at least 80% of the DNA had a M_w/M_n ratio smaller than 1.1 and was characterized by a M_w of 96.500 (146 base pairs). The ratio of the optical absorbances A_{260}/A_{280} is 1.80, indicating that the material was essentially free of protein.[13] Hyperchromic effects were always greater than 30%, which is commonly taken to indicate that the DNA fragments were not denatured during the dialysis. This does not mean that the DNA is flawless in the sense of a complete absence of partial premelting effects. In previous work,[5] indications for premelting were found in the whole temperature range from 278 to 338 K. With the use of atomic absorption spectroscopy, the sodium ion content of the DNA was determined to be 98%.

NMR tubes (5 mm diameter) were heated in $NaHCO_3$ and EDTA solutions to remove ionic impurities. Afterwards the tubes were extensively rinsed with water and dried in a vacuum oven. Quartz tubes were used to minimize small ion contamination due to leakage from the glass.

Samples were prepared by dissolving sodium DNA in water without adding extra low molecular weight salt. Concentrations were determined by weight. For this purpose, the water content

of the freeze dried material was determined by IR spectroscopy. The concentration of sample 1 was 44 mg/mL (i.e., 0.13 mol nucleotides/L), whereas the concentration of sample 2 amounted to 153 mg/mL (0.46 mol nucleotides/L). For multiple-pulse quadrupole echo experiments, a third sample was prepared with a concentration of 13 mg/mL (0.039 mol nucleotides/L). Samples 1 and 3 are transparent and isotropic. Sample 2 is birefringent and clearly liquid crystalline. These samples will be referred to as isotropic and anisotropic, respectively.

Longitudinal and transverse relaxation measurements were performed on three different spectrometers, i.e., two homebuilt and one Bruker MSL-400. In each experiment, 128 points were taken. The applied magnetic field strengths were 2.1, 6.3, and 9.3 T, respectively. These field strengths correspond to sodium Larmor frequencies of 23.7, 71.4, and 105.8 MHz. To check for a possible distribution in static quadrupole splitting, two-dimensional quadrupole echo experiments were performed on the MSL-400 and the homebuilt 6.3 T spectrometer. Furthermore, for sample 3 the low-frequency behavior of the spectral density was investigated using the multiple-pulse quadrupole echo method on the MSL-400.

The superconducting 6.3 and 9.3 T magnets have their field aligned along the sample tube, whereas the direction of the 2.1 T electromagnet field is perpendicular to the tube. In the latter case, the temperature was calibrated using a thermometer which could be inserted directly at the sample position and controlled by a fluid thermostat using fluorinert FC-43 (3M Co.). In this way, the accuracy of the temperature was within ±0.2 K. In the former case, the temperature was measured using the temperature-sensitive shift of tetramethylammonium in a H_2O/D_2O mixture.[14] In this configuration, the temperature was controlled by a gas thermostat (Bruker BVT 1000) within ±0.5 K.

Longitudinal and transverse relaxation rates were measured at temperatures varying from 278 to 303 K with increments of 5 K. To investigate the melting behavior in both samples, relaxation rates were measured up to 363 K at a field strength of 6.3 T. Quadrupole echo experiments were performed at 278, 283, 298, and 303 K on the MSL-400. On the 6.3 T spectrometer, these experiments were performed at 293 and 298 K. The multiple-pulse relaxation rates were determined at 283 and 298 K. In these experiments, the $\pi/2$ pulse duration was 15 μs and the pulse cycle time was varied from 115 to 3015 μs and from 115 to 5015 μs, respectively.

Longitudinal relaxation rates have been determined using the pulse-alternated inversion-recovery method.[15] Transverse relaxation rates have been measured by the spin-echo method, employing exorcycle phase cycling.[16] Two-dimensional quadrupole echo experiments are detailed in ref 9 and for multiple-pulse quadrupole echo experiments the reader is referred to ref 7.

In the case of the isotropic samples, free induction decays (fids) were sampled in the time domain and the relaxation curves were fitted with a sum of two exponentials with fixed fractions (see Theory section). Due to a nonzero average electric field gradient, in the liquid-crystalline solution the sodium spectrum shows a resolved static quadrupole splitting. Therefore, the relaxation behavior of both the central and the satellite peaks can be evaluated. Fids were Fourier transformed with respect to the detection time ($F(\omega_2)$ domain) to separate the different peaks. To construct T_1-relaxation curves each peak was integrated. The obtained curves were fitted with either one or two exponentials, according to the theoretical equations mentioned before. To determine the transverse relaxation rates of sample 2, the data were Fourier transformed with respect to both the detection time as well as the spin-echo evolution time ($F(\omega_1)$ domain). On resonance, a two-dimensional plot of the spectrum shows the central peak in the middle and the two satellites on the diagonal symmetrically located about the central line. The signals can be fitted with a single Lorentzian in the $F(\omega)_i$ domain. The characteristic width of this Lorentzian times π equals the transverse relaxation rate.

The data treatment of the quadrupole echo experiment is exactly similar to the transverse relaxation experiment. In the $F(\omega_i)$-domain satellite peaks appear not only at their usual position but also at the resonance frequency. The characteristic width of the latter peaks is insensitive to a distribution in quadrupole splitting.

All fits were performed using a non-linear least-squares procedure.[17] Each experiment was carried out several times depending on the signal-to-noise ratio, but at least in duplo. This resulted in an estimated reproducibility in rates within 5%. This accuracy applies to duplicate measurements on the same sample and to different samples of the same DNA preparation.

The estimated error margin in the calculated spectral densities is about ±8 s^{-1} and in the quadrupole splittings about 2%. The errors in the correlation times and coupling constants were evaluated by error propagation using multivariate error analysis[17] and are given in Table 4, a and b.

Results and Discussion

All relaxation rates of the isotropic and the anisotropic sample at three different field strengths in the temperature range 278 to 303 K are collected in Table 1, parts a and b, respectively. In both phases the relaxation was out of the extreme narrowing limit. Moreover, in the anisotropic sample the sodium resonance showed a quadrupole splitting. The integrated intensity of the central peak relates to that of the satellites as 3:4, indicating that the sample was completely liquid-crystalline.

All relaxation rates decrease with increasing temperature as has been reported before for similar DNA fragment solutions.[2,5] In the work of van Dijk et al.,[5] relaxation measurements were performed on salt free, isotropic solutions of similar DNA fragments, but at a lower concentration (0.07 M). The reported relaxation rates were somewhat lower compared to those in the present work.

Figure 1, a and b, shows the logarithm of the relaxation rates of both the isotropic and the anisotropic sample, respectively, vs the inverse temperature at a field strength of 6.3 T, corresponding to a sodium resonance frequency of 71.4 MHz. It is known that the relaxation rates decrease rapidly if the DNA starts to melt.[5] The spectral density function is analyzed in the temperature interval 278 to 303 K. In this interval the sharp decrease of the relaxation rates which is characteristic for melting is not observed. The relaxation rates decrease smoothly with increasing temperature and eventually approach the extreme narrowing limit, i.e., $J_0(0) = J_1(\omega_0) = J_2(2\omega_0)$. This smooth decrease of the relaxation rates before the actual melting range is interpreted as premelting.[5] These global features are the same at the other two field strengths. Polarized light microscopy showed no change in texture in this temperature interval.

In the isotropic sample, the melting traject starts at about 338 K, whereas in the liquid crystal the onset of melting seems to be at a somewhat lower temperature, say 328 K. However, at this temperature the satellites are no longer clearly resolved from the central peak and, accordingly, global averaged R_1 and R_2 values are obtained. Observing the melting ranges, it can be concluded that the actual melting temperature probably does not substantially change in the present concentration range. Similar behavior has been observed by infrared spectroscopy experiments.[18] Here, the melting traject of a 100 mg/mL calf thymus DNA solution in D_2O with 0.15 M KCl has been compared with the melting traject of a 0.04 mg/mL DNA solution in H_2O (0.15 M NaCl,

TABLE 1: (a) Relaxation Rates (s^{-1}) of the Isotropic Sample (a) and Anisotropic Sample (b) at Different Temperatures and Larmor Frequencies[a]

		23.7 MHz	71.4 MHz	105.8 MHz
		(a) Isotropic Sample		
278 K	R_{1f}	356	210	130
	R_{1s}	218	146	105
	R_{2f}	593	359	176
	R_{2s}	225	176	149
283 K	R_{1f}	296	189	143
	R_{1s}	184	129	98
	R_{2f}	504	297	273
	R_{2s}	206	161	136
288 K	R_{1f}	226	166	140
	R_{1s}	161	115	82
	R_{2f}	423	240	229
	R_{2s}	181	144	134
293 K	R_{1f}	194	137	126
	R_{1s}	134	103	81
	R_{2f}	322	193	229
	R_{2s}	152	126	100
298 K	R_{1f}	198	124	110
	R_{1s}	111	93	72
	R_{2f}	233	165	148
	R_{2s}	142	110	100
303 K	R_{1f}	141	103	109
	R_{1s}	93	85	69
	R_{2f}	163	143	161
	R_{2s}	117	95	87
		(b) Anisotropic Sample		
278 K	R_{1f}^c	348	217	166
	R_{1s}^c		174	124
	R_1^s	290	172	129
	R_2^c	319	209	161
	R_2^s	552	464	337
283 K	R_{1f}^c	291	190	163
	R_{1s}^c		156	103
	R_1^s	262	154	112
	R_2^c	269	183	150
	R_2^s	448	382	277
288 K	R_{1f}^c	241	168	153
	R_{1s}^c		142	94
	R_1^s	232	139	105
	R_2^c	235	162	144
	R_2^s	392	312	241
293 K	R_{1f}^c	205	149	136
	R_{1s}^c		127	89
	R_1^s	201	126	97
	R_2^c	194	143	114
	R_2^s	319	276	213
298 K	R_{1f}^c	176	134	128
	R_{1s}^c		109	82
	R_1^s	177	112	88
	R_2^c	167	129	114
	R_2^s	265	221	184
303 K	R_{1f}^c	147	115	118
	R_{1s}^c		102	78
	R_1^s	151	102	81
	R_2^c	143	118	104
	R_2^s	265	192	162

[a] The estimated error is about 5%.

0.015 M sodium citrate), as monitored by the ultraviolet method. In this concentration range, no substantial difference in melting traject and actual melting temperature was found.

In the isotropic solution, both the longitudinal and transverse relaxations are biexponential. Using eqs 1–4 the spectral densities were calculated. Four different relaxation rates per field strength resulted in 12 dependent equations with 7 unknown spectral density functions. These spectral densities include the values at zero frequency, the Larmor frequency, and twice the Larmor frequency at all three different field strengths. The calculated spectral densities are shown in Table 2a.

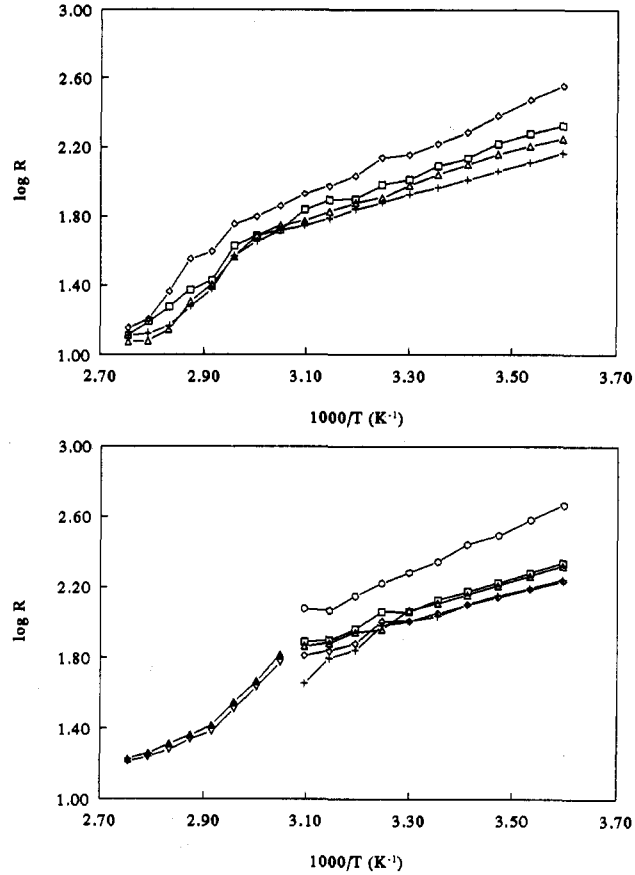

Figure 1. (a, top) Temperature dependence of the relaxation rates in the isotropic sample: (□) R_{1f}; (+) R_{1s}; (◇) R_{2f}; (△) R_{2s}. (b, bottom) Temperature dependence of the relaxation rates in the anisotropic sample: (□) R_{1f}^c; (+) R_{1s}^c; (◇) R_2^c; (△) R_1^s; (○) R_2^s; (▽) R_1; (▲) R_2.

TABLE 2: Spectral Densities (s^{-1}) at Different Frequencies (MHz) of the Isotropic Sample (a) and Anisotropic Sample (b) at Different Temperatures[a]

T (K)	$J(0)$	$J(24)$	$J(48)$	$J(71)$	$J(106)$	$J(143)$	$J(212)$
			(a) Isotropic Sample				
278	304	168	99	105	70	73	58
283	254	142	87	95	74	65	51
288	208	111	78	84	74	58	45
293	172	95	65	69	63	52	40
298	110	97	53	62	56	47	38
303	97	71	47	52	54	43	34
			(b) Anisotropic Sample				
278	223	189	145	111	86	88	65
283	171	149	131	97	84	79	55
288	140	122	116	85	80	71	51
293	118	99	101	76	68	64	46
298	89	83	89	68	65	56	43
303	75	70	75	59	60	52	40

[a] The estimated error margin is about ±8 s^{-1}.

Figure 2a shows the spectral density function at a number of temperatures in the isotropic case. From the multiple-pulse experiments (eqs 5–7; data not shown), it is concluded that there are no additional slow relaxation processes in a 13 mg/mL isotropic solution in the frequency range 200–9000 Hz. At both 283 and 298 K, the spectral density $J_{20}(T)$ did not vary with the pulse cycle time (see experimental section). Moreover, $J_{20}(T)$ equaled $J_0(0)$, the latter being determined from longitudinal and transverse relaxation measurements. These results, together with the fact that all spectral densities show smooth behavior at low frequencies (Figure 2a), lead to the conclusion that, also in the 44 mg/mL isotropic solution, no additional slow dynamical processes in the frequency range 200–9000 Hz are present at all temperatures.

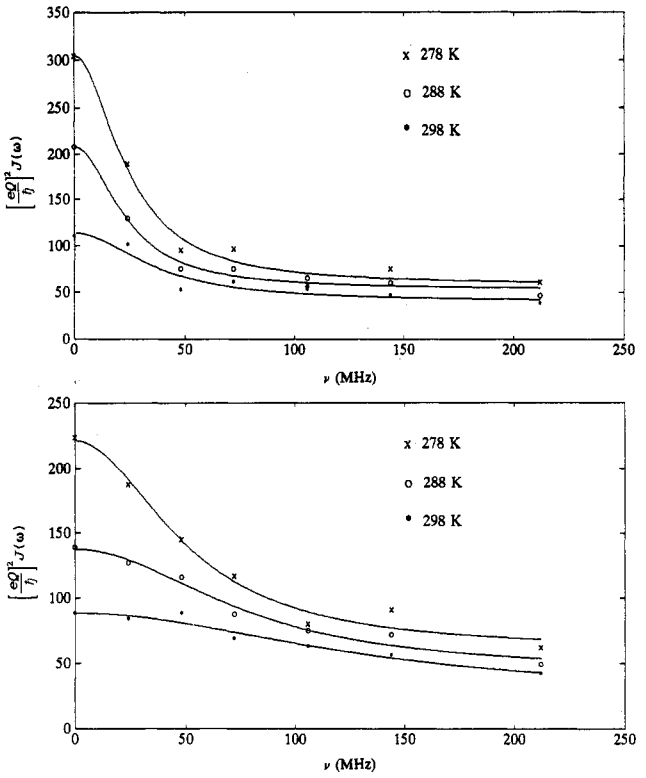

Figure 2. (a, top) Effect of temperature on the spectral density in the isotropic sample. (b, bottom) Effect of temperature on the spectral density in the anisotropic sample.

TABLE 3: Temperature Dependence of the Quadrupole Splitting at Different Larmor Frequencies[a]

T (K)	ω_Q (Hz) ω_0 = 24 MHz	ω_Q (Hz) ω_0 = 71 MHz	ω_Q (Hz) ω_0 = 106 MHz
278	859	872	772
283	755	791	706
288	664	684	645
293	596	619	580
298	572	516	514
303	459	439	459

[a] The estimated error is about 2%.

In the anisotropic solution, the sodium resonance showed a quadrupole splitting. In Table 3, the temperature and field dependence of the quadrupole splitting is listed. This splitting decreases linearly with increasing temperature and shows no clear magnetic field dependence in the range from 2.1 to 6.3 T. In a cholesteric liquid-crystalline DNA solution, the DNA fragments tend to align perpendicular to the external magnetic field. At a field strength of 2.1 T the magnetic field was perpendicular to the NMR tube axis, whereas for the other field strengths the field was directed parallel to this axis. No difference in quadrupole splitting was observed.

The quadrupole splitting shows a similar temperature dependence as has been reported by Strzelecka et al.[2] If we extrapolate their data to a concentration of about 150 mg/mL, the quadrupole splitting is somewhat lower than in our case (about 25% at 293 K). However, they observed no quadrupole splitting at all at concentrations below 180 mg/mL. At about 150 mg/mL they characterized the phase of the solution to consist of an isotropic and a precholesteric part. It should be noted, though, that their solutions contained about 0.01 M excess low molecular weight salt. Moreover, Wang et al.[19] investigated salt-free DNA solutions with a concentration up to 182 mg/mL by small-angle X-ray scattering and observed no indication of anisotropy. The observation of a single broad peak with no evidence of multiple peaks was the main reason for this conclusion. However, even in a visibly birefringent liquid-crystalline solution of DNA fragments (about 285 mg/mL), only one broad peak is observed in a q range from 0.02 to 0.22 Å^{-1} (small-angle neutron scattering results, Groot et al., to be published).

To check this difference in phase behavior, the sample preparation was repeated four times and no change of results was observed. As mentioned before, the solutions of Strzelecka et al.[2] contained about 0.01 M excess low molecular weight salt. Both Strzelecka et al.[2] and Wang et al.[19] used calf thymus DNA, whereas in the present work chicken erythrocyte nucleosome core DNA was used. This, together with a possible difference in molecular weight distribution, is the most likely cause of the difference in phase behavior.

In the liquid-crystalline solution, the quadrupole splitting appeared to be homogeneous throughout the sample. Satellite signals at $\omega_1 = 0$ in the $F(\omega_1)$ domain, obtained using the quadrupolar echo sequence,[9] have the same width as the usual satellites, observed in transverse relaxation experiments (data not shown). Since the former satellite signals are essentially free of line-broadening effects due to an inhomogeneous ω_Q, it is concluded that the quadrupole splitting is uniform.

Since in the anisotropic sample the sodium resonance shows a substantial quadrupolar splitting (ω_Q exceeds at least 5 times the characteristic line width), relaxation rates of both the central peak and the satellites could be determined. Except at a field strength of 2.1 T, the longitudinal relaxation of the central peak could be fitted to a sum of two exponentials. Using eqs 9–16 the spectral densities were calculated. This resulted in 14 different equations with the aforementioned 7 unknown spectral densities. The results are collected in Table 2b.

In Figure 2b, the spectral density in the anisotropic sample at a number of temperatures is shown. Similar to the isotropic case, in the low-frequency range the spectral density is a smooth function. Accordingly, it is concluded that, also in the anisotropic phase, there are no slowly fluctuating processes that drive the relaxation in the microsecond time scale, like, for instance, director fluctuations.

The spatial orientation dependence of the electric field gradient correlation function (i.e., the dependence on the index m in eq 17) can be checked by comparing the spectral densities $J_1(\omega)$ and $J_2(2\omega')$ under the condition $\omega = 2\omega'$. This can be realized by performing experiments at two magnetic field strengths which differ exactly a factor of 2. Unfortunately, in the present situation this condition is never fulfilled (B_0 = 2.1, 6.3, and 9.3 T). However, the anisotropic sample spectral densities show a relatively smooth behavior with respect to the frequency (Figure 2b) and this behavior is similar to the situation in an isotropic sample (Figure 2a). Accordingly, any spatial orientation dependence of the electric field gradient tensor correlation function is beyond observation and, hence, will be neglected.

For both the isotropic and the anisotropic cases, the resulting spectral densities can be fitted to a sum of a Lorentzian and a constant:

$$\left[\frac{eQ}{\hbar}\right]^2 J(\omega) = \frac{A\tau_1}{1 + \omega^2\tau_1^2} + B \qquad (21)$$

where τ_1 denotes the correlation time for the slow relaxation process. The constant A comprises the corresponding coupling constant χ_1, according to $A = (\pi^2/5)\langle\chi_1^2\rangle$. The constant B may be identified with a second Lorentzian with a very short characteristic correlation time with respect to the inverse Larmor frequency: $B = (\pi^2/5)\langle\chi_2^2\rangle\tau_2$.

The sodium ion relaxation behavior is caused by interaction of the nuclear electric quadrupole moment with fluctuating electric field gradients generated by the surrounding medium. The negatively charged phosphates on the DNA backbone and the water molecules are the most likely candidates to produce such field gradients. Since in general the water dynamics is (much)

TABLE 4: Temperature Dependence of the Correlation Times and Coupling Constants of the Isotropic Sample (a) and Anisotropic Sample (b)

T (K)	τ_1 (ns)	$\langle\chi_1^2\rangle^{1/2}$ (kHz)	$\langle\chi_2^2\rangle\,\tau_2$ (Hz)
	(a) Isotropic Sample		
278	7.5 ± 0.9	126 ± 8	33 ± 3
283	7.7 ± 1.1	112 ± 9	32 ± 3
288	8.6 ± 1.8	93 ± 10	30 ± 3
293	8.5 ± 1.6	85 ± 9	26 ± 3
298	4.5 ± 1.4	89 ± 15	21 ± 3
303	6.5 ± 2.0	65 ± 11	21 ± 2
	(b) Anisotropic Sample		
278	3.3 ± 0.3	157 ± 8	31 ± 3
283	2.5 ± 0.4	155 ± 12	26 ± 4
288	2.1 ± 0.4	148 ± 17	23 ± 5
293	2.0 ± 0.5	136 ± 20	21 ± 5
298	1.2 ± 0.4	164 ± 33	13 ± 8
303	1.0 ± 0.4	164 ± 48	11 ± 11

faster than the macromolecule dynamics, the slow process is most likely concerned with the interaction between the sodium counterions and the DNA. The low field dispersion could be a direct electrostatic effect of the counterion–DNA interaction and/or a solvent-mediated effect due to the disturbance of the counterion solvation sheath. The fast process is most likely due to the influence of the relatively fast water dynamics.

Table 4, a and b, contains the coupling constants and correlation times for the isotropic and the anisotropic sample, respectively, at various temperatures. On comparing the correlation times and the coupling constants of the slow relaxation process in both phases, several remarkable differences are observed. In the isotropic phase, no clear temperature dependence beyond the estimated error is observed with respect to the correlation time of the slow process τ_1. The corresponding coupling constant $\langle\chi_1^2\rangle^{1/2}$ decreases with increasing temperature. The anisotropic samples show more or less the opposite temperature behavior regarding the slow process. Here, the coupling constant seems to be unaffected by temperature and the correlation time τ_1 decreases with increasing temperature. In both phases the fast process contribution decreases while raising the temperature.

Apart from the temperature behavior, the values of the various parameters in both phases may be compared. For the isotropic sample, the correlation time τ_1 is larger than is observed for the anisotropic sample. The coupling constant $\langle\chi_1^2\rangle^{1/2}$ is somewhat larger in the anisotropic case. In the isotropic situation, the contribution of the fast process $\langle\chi_2^2\rangle\tau_2$ seems to be systematically higher than in the anisotropic case, although the difference is of the order of the estimated error margins.

The results obtained in the isotropic sample can be compared to previously reported results on a less concentrated solution (0.07 vs 0.13 M). Van Dijk et al.[5] observed similar coupling constants. The correlation times τ_1 were somewhat smaller and decreased with increasing temperature. In the latter work, however, the estimated error margins in τ_1 are significantly smaller. This is due to the fact that in van Dijk's work more data in the low frequency range (4–16 MHz) were collected. Accordingly, in the present contribution a similar decrease in τ_1 would be beyond observation. The difference in correlation time magnitude is most likely related to the difference in concentration.

In the isotropic phase, $\langle\chi_1^2\rangle^{1/2}$ decreases relatively sharply with increasing temperature, whereas no substantial temperature dependence is observed in the temperature interval 278–303 K in the anisotropic solution. According to the condensation concept of Manning[20] and Oosawa,[21] a fraction of $1 - \xi^{-1}$ (ξ being the linear charge density parameter) of counterions will condense. For the present DNA solutions, this fraction is about 0.76. If only the effect of temperature is included, this fraction will decrease about 2% on raising the temperature from 278 to 303 K. Obviously, this effect cannot fully explain the observed decrease of $\langle\chi_1^2\rangle^{1/2}$ on raising the temperature. It has been reported before[5] that a decrease of the coupling constant with increasing temperature indicates premelting of the DNA. If premelting occurs, the charge density on the DNA backbone decreases and, as a consequence, the direct interaction between the counterions and the DNA diminishes, resulting in a smaller coupling constant. Apparently, the DNA is stabilized in a liquid-crystalline phase, because here $\langle\chi_1^2\rangle^{1/2}$ takes larger values and shows no substantial temperature dependence. This may be due to increased screening of the electrostatic repulsion of the phosphate groups induced by the higher ionic strength.

The behavior of the correlation time τ_1 in both phases is consistent with the tentative explanation of the different temperature dependencies of the coupling constant $\langle\chi_1^2\rangle^{1/2}$. Due to premelting the DNA molecule is no longer a rigid rod producing a cylindrically symmetric electric field gradient which is easily averaged locally. Some parts of the DNA helix may be flawed, so in general the counterion has to diffuse a longer time near the DNA molecule to average out the experienced electric field gradient. The latter time may be identified with the correlation time τ_1. Accordingly, in the isotropic phase larger values for τ_1 are observed, since in the latter system premelting effects are more manifested.

Apart from premelting effects, the correlation time τ_1 may be sensitive to the counterion diffusion. Accordingly, in the anisotropic phase (where no premelting effects were observed) the observed temperature dependence of τ_1 is probably related to a temperature-dependent sodium diffusion. In the isotropic solution, no temperature dependence in τ_1 could be observed. As stated before, here a possible temperature effect (as reported in previous work[5]) can easily escape observation due to the substantial error margins. Another explanation is the fact that in the isotropic phase the effect of a temperature-dependent counterion diffusion is compensated by premelting effects.

The effect of the concentration and/or phase of the DNA solutions on the self-diffusion coefficient of the sodium ion is not very large. In the isotropic phase this coefficient is 7×10^{-6} cm^2/s, whereas the corresponding value in the anisotropic phase equals 6×10^{-6} cm^2/s (unpublished results). Accordingly, the estimated root mean square displacement of a counterion within the typical values of the correlation time τ_1 is of the order of 5 nm in both phases. Since the cholesteric pitch is 3 orders of magnitude larger, possible changes in the macroscopic organization are not expected to have a large effect on the spin relaxation. Changes in the local (molecular) structure, however, may have a profound influence on the relaxation behavior.

In previous work, the long correlation time was interpreted using the simple model by van der Klink et al.[22] Using this model, the influence of the concentration difference in the isotropic and anisotropic systems on the correlation time may be estimated. This effect turns out to be very small, i.e., of the order of 5% and therefore can not account for the present observations.

Conclusions

In the present work, a salt-free 153 mg/mL DNA solution appeared to be fully liquid-crystalline, whereas in previous work[2,19] solutions of that concentration were found to be isotropic and/or precholesteric. This indicates that the phase behavior of persistence length DNA fragment solutions may depend substantially on the origin and/or the molecular weight distribution of the DNA fragments, in addition to the presence of supporting electrolyte.

In the anisotropic phase, the sodium resonance shows a quadrupolar splitting. The splitting is homogeneous throughout the sample, indicating that the director is uniformly oriented perpendicular to the magnetic field. The orientation distribution of individual DNA fragments with respect to the director has been investigated using SANS and will be published elsewhere. The substantial splittings allow for the determination of relaxation

rates of both the central transition and the satellites from which the dynamic information is derived.

The relaxation behavior of the sodium counterions in isotropic and anisotropic, liquid-crystalline DNA solutions is caused by, at least, two processes on different time scales. One relatively fast process is most likely due to the fast water dynamics in the solutions. The (inseparable) product of the squared coupling constant and the correlation time, $\langle\chi_2^2\rangle\tau_2$, is of the order of 15–30 Hz for both phases. The other process occurs on a much larger time scale and is presumably caused by diffusion of the counterions near the DNA. The correlation time τ_1 is of the order of 7 ns in the isotropic solution and about 2 ns in the anisotropic situation. The corresponding value of the coupling constant $\langle\chi_1^2\rangle^{1/2}$ is of the order of 95 or 150 kHz for the isotropic and anisotropic sample, respectively. No additional slowly fluctuating processes in the frequency range 200–9000 Hz were observed.

The values of the slow process coupling constants and correlation times, together with their respective temperature behavior, indicate premelting in the isotropic solution. In the liquid-crystalline solutions, this effect has not been observed. These results confirm that spin relaxation is more or less dominated by local effects on the molecular distance scale. Apart from the effects on the molecular structure, the macroscopic organization does not have a large influence on the counterion relaxation rates. This can be assessed on the fact that the root mean square displacement of an ion within the typical values of the correlation time τ_1 is of the order of 5 nm, three orders of magnitude smaller than the cholesteric pitch. Moreover, polarized light microscopy shows no change in texture in the present temperature interval.

The fact that the quite similar decrease of the relaxation rates with increasing temperatures in both phases has different origins (i.e., the decrease of the coupling constant in the isotropic phase and the decrease of the correlation time in the anisotropic phase) emphasizes the importance of field-dependent measurements.

References and Notes

(1) Strzelecka, T. E.; Rill, R. L. *Macromolecules* **1991**, *24*, 5124.
(2) Strzelecka, T. E.; Rill, R. L. *Biopolymers* **1990**, *30*, 803.
(3) Livolant, F. *J. Physique* **1987**, *48*, 1051.
(4) Livolant, F.; Levelut, A. M.; Doucet, J.; Benoit, J. P. *Nature* **1989**, *339*, 724.
(5) van Dijk, L.; Gruwel, M. L. H.; Jesse, W.; de Bleijser, J.; Leyte, J. C. *Biopolymers* **1987**, *46*, 261.
(6) Hubbard, P. S. *J. Chem. Phys.* **1970**, *53*, 985.
(7) van der Maarel, J. R. C. *J. Chem. Phys.* **1991**, *94*, 4765.
(8) van der Maarel, J. R. C. *Chem. Phys. Lett.* **1989**, *155*, 288.
(9) Furo, I.; Halle, B.; Wong, T. C. *J. Chem. Phys.* **1988**, *89*, 5382.
(10) Ernst, R. R.; Bodenhausen, G.; Wokaun, A. *Principles of Nuclear Magnetic Resonance in One and Two Dimensions*; Oxford University Press: London, 1987.
(11) Shindo, H.; McGhee, J. D.; Cohen, J. S. *Biopolymers* **1980**, *19*, 523.
(12) Nicolai, T.; van Dijk, L.; van Dijk; J. A. P. P.; Smit, J. A. M. *J. Chromatogr.* **1987**, *389*, 286.
(13) Liebe, D. C.; Stuehr, J. E. *Biopolymers* **1972**, *11*, 167.
(14) Hartel, A. J.; Lankhorst, P. P.; Altona, C. *Eur. J. Biochem.* **1982**, *129*, 343. (Note: the constant *a* for the lower temperature range mentioned on p 346 should be 177.6 instead of 179, private communication.)
(15) Demco, D. E.; van Hecke, P.; Waugh, J. S. *J. Magn. Reson.* **1974**, *16*, 467.
(16) Bodenhausen, G.; Freeman, R.; Turner, D. L. *J. Magn. Reson.* **1977**, *27*, 511.
(17) Clifford, A. A. *Multivariate Error Analysis*; Applied Science Publishers Ltd.: London, 1973.
(18) Fritsche, H. *Biochim. Biophys. Acta* **1966**, *119*, 645.
(19) Wang, L.; Bloomfield, V. A. *Macromolecules* **1991**, *24*, 5791.
(20) Manning, G. S. *J. Chem. Phys.* **1969**, *51*, 924.
(21) Oosawa, F. *Polyelectrolytes*; Dekker: New York, 1971.
(22) van der Klink, J. J.; Zuiderweg, L. H.; Leyte, J. C. *J. Chem. Phys.* **1974**, *60*, 2391.